Metagenomic sequencing provides insights into the location of microbial detoxification in the gut of a small mammalian herbivore

Running title: *Determining the site of microbial detoxification*

Kevin D. Kohl[1,2], Kelly F. Oakeson[2], Teri J. Orr[2], Aaron W. Miller[2,3], Jennifer Sorensen Forbey[4], Caleb D. Phillips[5], Colin Dale[2], Robert B. Weiss[6], M. Denise Dearing[2]

[1]*Department of Biological Sciences, University of Pittsburgh, 4249 Fifth Ave., Pittsburgh, PA, 15260, USA*

[2] *Department of Biology, University of Utah, 257 South 1400 East, Salt Lake City, UT, 84112, USA*

[3] *Departments of Urology and Immunology, Cleveland Clinic Foundation, 9500 Euclid Ave, Cleveland, OH 44195*

[4] Department of Biological Sciences, Boise State University, 1910 University Drive, Boise, Idaho 83725 USA

[5] *Department of Biological Sciences, Texas Tech University, 2901 Main Street, Lubbock, TX, 79409*

[6] *Department of Human Genetics, University of Utah, 15 North 2030 East, Salt Lake City, UT, 84112, USA*

Corresponding Author:

Kevin Kohl – University of Pittsburgh

Kevin.d.kohl@gmail.com

Abstract – Microbial detoxification of plant defense compounds influences the use of certain plants as food sources by herbivores. The location of microbial detoxification along the gut could have profound influences on the distribution, metabolism, and tolerance to toxic compounds. Stephen's woodrats (*Neotoma stephensi*) specialize on juniper, which is heavily defended by numerous defensive compounds, such as oxalate, phenolics, and monoterpenes. Woodrats maintain two gut chambers harboring dense microbial communities: a foregut chamber proximal to the major site of toxin absorption, and a cecal chamber in their hindgut. First, we conducted a trial with antibiotics to determine whether the gut microbiota is important in allowing *N. stephensi* to consume juniper. Antibiotic-treated animals lost significantly more body mass while feeding on juniper, relative to those feeding on rabbit chow. Next, we measured levels of toxins throughout the gut. Oxalate concentrations were immediately lower in the foregut chamber, while concentrations of terpenes remain high in the foregut, and are lowest in the cecal chamber. Finally, we conducted metagenomic sequencing of the foregut and cecal chambers. We found that the majority of genes associated with detoxification functions were more abundant in the cecal chamber. However, some genes associated with degradation of oxalate and phenolic compounds were more abundant in the foregut. Thus, it seems that microbial detoxification may take place in various chambers depending on the class of chemical compound. We hypothesize that the location of microbial detoxification could impact the tolerance of animals to these compounds, which may have ecological and evolutionary consequences.

Importance – For decades, ecologists have investigated how partnerships with fermentative microbes have contributed to the success of mammalian herbivores. The location of these partnerships in the gut (foregut vs. hindgut fermentation) can have large implications for host ecology, such as limiting body size or dietary niche breadth. Mammalian herbivores also host microbial communities that aid in the detoxification of plant defensive compounds, though the location of these functions in the gut has not been studied thoroughly. Here, we used metagenomic sequencing to investigate the location of detoxification functions in the gut of a small mammalian herbivore, Stephen's woodrat, which has both a foregut and a hindgut chamber. We found that most detoxification genes exhibited higher abundance in the hindgut, though genes associated with oxalate degradation were enriched in the foregut. We hypothesize that similar to microbial fermentation, the location of microbial detoxification may also have implications for host ecology.

73 **INTRODUCTION**

74 Mammalian herbivores are often challenged by the consumption of toxic
75 plant secondary compounds (PSCs) that negatively impact their physiology in
76 various ways (1). In response, mammalian herbivores have evolved myriad
77 adaptations to cope with dietary toxins, such as altered behavior, efflux pumps in
78 the gut, and enhanced liver detoxification (1). Recently, we demonstrated that the
79 gut microbiota of herbivores also play an important role in allowing them to
80 consume PSCs (2). However, it is still unclear where the process of microbial
81 detoxification occurs in the gut.

82 It has been proposed that microbial detoxification should occur early in the
83 gastrointestinal tract, to facilitate rapid degradation of PSCs and minimize the
84 potential for their absorption in the digestive tract. In fact, it has been hypothesized
85 that the rumen evolved first for detoxification and was later adopted for processes
86 of fermentation (3, 4). Examples of animals in which foregut detoxification has been
87 documented for particular PSCs include reindeer (*Rangifer tarandus*; (5) that have
88 rumen communities that degrade usnic acid, a toxin produced by lichen, and
89 hoatzins (*Opisthocomus hoazin*), that maintain communities of microbes in their
90 foregut capable of metabolizing saponins (6). There is also evidence of microbial
91 detoxification processes occurring in the hindguts of some animals. For example,
92 Sage-grouse (*Centrocercus urophasianus*), specialize on toxic sagebrush (*Artemsia*
93 spp.) and maintain a cecal microbiota enriched in detoxification genes (7).
94 Additionally, the hindguts of koalas (*Phascolarctos cinereus*) harbor microbes
95 capable of degrading phenolic PSCs (8). Understanding the location of microbial

processes in the gut is likely to be important in the context of animal ecology. For example, the location of fermentation (foregut vs hindgut), seems to facilitate or constrain evolution of herbivore body size (9) and dietary niche breadth (10). The location of microbial detoxification could have similar impacts on animal ecology.

In contrast to many above described examples, woodrats (genus *Neotoma*) are particularly interesting from a digestive standpoint as these herbivorous rodents possess both a foregut chamber and a large cecal chamber in their hindgut. Both the foregut and cecal chambers harbor dense communities of microbes and high concentrations of volatile fatty acids (11), which are the microbial products of fermentation. Following the hypothesis that the bovine rumen first evolved for detoxification regarding the rumen (3, 4), we predict that microbial detoxification of PSCs might occur prior to the small intestine in the woodrat gut such that the animal experiences limited absorption and systemic exposure to toxic compounds.

To evaluate this hypothesis, we conducted a series of experiments focusing on a species of woodrat with a highly specialized diet. Stephen's woodrat (*Neotoma stephensi*) is a dietary specialist, with juniper (*Juniperus monosperma*) composing ~90% of its diet (12). Juniper defends itself from herbivory with various toxic compounds, including monoterpenes (13), phenolics (14, 15), and oxalate (16). We have demonstrated that microbes aid in the detoxification of phenolics (2) and oxalate in other woodrat species (17, 18). For example, some populations of the white-throated woodrat (*N. albigula*) specialize on cactus (*Opuntia* spp.), which is rich in oxalate, but lacking in other defensive compounds. The foregut microbial communities of these *N. albigula* contain several species of oxalate-degrading

119 microbes (19). There has also been metagenomic evidence obtained from other
120 systems suggesting that microbes aid in the detoxification of terpenes (mountain
121 pine beetles: (20); sage grouse: (7), as well as experimental work demonstrating the
122 detoxification function of the gut microbiota of pine weevils (21). However, the
123 detoxification contribution of the microbiome has not been compared between the
124 foregut and hindgut in any wild vertebrate herbivore.

125 We addressed several questions within the woodrat-juniper system. First, to
126 determine if the gut microbiota plays a role in facilitating the consumption of
127 juniper we conducted a feeding trial with *N. stephensi* where we disrupted the
128 microbial community with antibiotics. We predicted that antibiotic treatments
129 would significantly impair the ability for *N. stephensi* to feed on juniper. Next, we
130 measured concentrations of two classes of toxins (oxalate and monoterpenes)
131 across regions of the gut. We predicted that if detoxification is occurring proximally
132 in the gut, then toxins concentrations in the foregut would be significantly lower
133 compared to food material. Last, we conducted a series of metagenomic analyses to
134 inventory and compare the functions of microbial communities. We first compared
135 the metagenomes of foregut communities between the juniper specialist *N. stephensi*
136 and the cactus specialist *N. albigula* and predicted that if the foregut microbiota of *N.*
137 *stephensi* were specialized for detoxification of juniper, which contains oxalate,
138 monoterpenes, and phenolics, we would observe enrichment of detoxification genes
139 compared to the foregut of *N. albigula* that is exposed primarily to the oxalate in
140 cactus. We also compared the metagenomes of foregut and cecal chambers within *N.*

141 *stephensi* and predicted that the metagenome of the foregut chamber would be
142 enriched in detoxification genes compared to the cecal communities.
143
144 **RESULTS**
145 *Antibiotic feeding trial*
146 Treatment with antibiotics significantly impaired the ability of *N. stephensi* to
147 feed on juniper-rich diets. Animals feeding on juniper exhibited a 9.5% decrease in
148 food intake when placed on antibiotics, while those feeding on a control diet only
149 decreased food intake by 2.4% (Fig. 1; Kruskal-Wallis: $P = 0.03$). This difference in
150 food intake corresponded to a difference in maintenance of body mass, such that
151 animals being fed a juniper diet lost roughly 6.3% of their body mass when placed
152 on antibiotics, while those fed the control diet only lost 1.5% of body mass (Fig. 1;
153 Kruskal-Wallis: $P = 0.03$).
154
155 *Concentrations of PSCs across the gut*
156 Water concentration varied over the length of the gut, with a significant
157 reduction in the large intestine (Fig. 2). Oxalate concentrations in the entire gut
158 were significantly less than in the food material (Fig 2; $P < 0.0001$). Oxalate
159 concentrations also varied significantly across gut regions ($P < 0.001$), and were
160 highest in the foregut and lowest in the stomach. Conversely, foregut concentrations
161 of monoterpenes were not significantly lower than the food material (Fig. 2; $P > 0.05$
162 for all). Concentrations of monoterpenes did vary across gut regions, with the

163 lowest concentrations always being in the cecum (Fig. 2; $P < 0.0001$ for all). In fact,
164 camphene and β-pinene were not detectable in any cecal samples.
165
166 *Metagenomic sequencing*
167 We obtained an average of 3.35 million reads per sample (± 517 thousand).
168 We first compared the bacterial metagenomes of foregut chambers from *N. stephensi*
169 (which specializes on juniper) and *N. albigula* (which specializes on cactus). There
170 were no functions that were significantly enriched in the foregut bacterial
171 metagenomes of *N. stephensi*. The foregut bacterial communities of *N. albigula* were
172 enriched in functions related to the metabolism of several amino acids and vitamin
173 B6 (Fig. 3). Further, when investigating detoxification genes, there were no
174 detectable differences between the two species.
175 We next searched for differential functions between the foregut and cecal
176 chambers of *N. stephensi*. The foregut bacterial metagenome was enriched in genes
177 associated with the metabolism of nucleotides (purines), amino acids (glutathione,
178 thiamine), vitamins (riboflavin, nicotinate, folate), and lipoic acid (Fig. 4A). The cecal
179 bacterial metagenome was enriched for genes associated with the metabolism of
180 starch and sucrose, as well as the biosynthesis of several essential amino acids (Fig.
181 4A). The cecum was also enriched in several functional categories related to
182 detoxification (drug metabolism, chloroalkane and chloroalkene degradation; Fig.
183 4A).
184 We also specifically investigated genes associated with "Xenobiotic
185 degradation and metabolism", "Geraniol degradation", and "Limonene and pinene

186 degradation". Here, the only gene enriched in the foregut was 4-oxalocrotonate
187 tautomerase, which was 24× more abundant in the foregut compared to the cecum
188 (Fig. 4B). There were 5 other detoxification genes that were significantly more
189 abundant in the cecum compared to the foregut chamber (Fig. 4B). Three of these
190 genes (carboxylesterase 2, hydroxyatrazine ethylaminohydrolase, and 2-
191 hydroxycyclohexanecarboxyl-CoA dehydrogenase) were 2-3× more abundant in the
192 cecal chambers compared to the foregut chambers. Two genes, anthraniloyl-CoA
193 monooxygenase and dehalogenases, were not detected in the foregut chambers, but
194 were present in the cecal chambers of the juniper-feeding *N. stephensi* (Fig. 4B).

195 Last, we focused on a subset of detoxification enzymes highlighted from
196 previous studies. The gene oxalyl-CoA decarboxylase, which is anticipated to
197 function in oxalate degradation, did not exhibit differential abundance between the
198 foregut chambers of *N. stephensi* and *N. albigula*. However, the abundance of this
199 gene was 4.5× higher in the foregut of *N. stephensi* compared to the cecum (Fig. 5).
200 Similarly, aryl-alcohol dehydrogenase, which is more abundant in the woodrat
201 foregut when animals are fed phenolic-rich creosote resin (2), did not exhibit
202 significant differences between the foregut chambers of *N. stephensi* or *N. albigula*,
203 but was 41× higher in the *N. stephensi* foregut compared to the cecum (Fig. 5). Last,
204 we investigated several genes in the "Limonene and pinene degradation" pathway,
205 which are enriched in other herbivores that feed on terpene-rich plants (7, 20, 21).
206 Enoyl-CoA hydratase (E.C. 4.2.1.17) was more abundant in the foregut of *N.*
207 *stephensi* compared to *N. albigula*, with no difference between the foregut and cecal
208 chambers of *N. stephensi* (Fig. 5). Additionally, aldehyde dehydrogenase (E.C.

209 1.2.1.3) exhibited no difference between the foregut chambers of *N. stephensi* and *N.*
210 *albigula,* but was 2.5× more abundant in the cecal chambers of *N. stephensi* (Fig. 5).

211 We found a significant positive relationship between the relative abundances
212 of functional categories as estimated by PICRUSt and determined by metagenomic
213 sequencing (Fig. 6; foregut: $R^2 = 0.49$, slope = 0.922 ± 0.074, $P < 0.0001$; cecum: $R^2 =$
214 0.51, slope = 0.978 ± 0.072, $P < 0.0001$). Some functional categories, such as those
215 representing 'Peptidases' and 'Amino acid Related Enzymes', were not well
216 predicted by PICRUSt, in that they were present on the x-axis (predicted to be
217 present by PICRUSt but not detected by metagenomic sequencing). However,
218 categories that exhibited the greatest fold-differences between the two chambers
219 were also predicted to differ by PICRUSt (Fig. 6; with the exception of Starch and
220 Sucrose Metabolism). Following assignment into functional community categories it
221 was determined that benzoate degradation abundance and the composition of its
222 contributing microbial lineages was significantly conserved (FDR adjusted p-value =
223 0.048) between the two chambers. Further investigations revealed that conserved
224 benzoate degradation function across chambers was contributed by a combination
225 of 28 different bacterial OTUs classified into eight genera (*Supplementary material).*

226 **DISCUSSION**

227 Here, we investigated the nature and location of microbial detoxification in
228 the guts of Stephen's woodrat, a juniper specialist. We found that microbes are
229 instrumental in allowing *N. stephensi* to feed on a diet of juniper. The location of
230 detoxification within the gut seems to vary depending on the chemical class of
231 defensive compounds. We discuss our findings below, as well as the potential

232 ecological and evolutionary consequences of foregut vs hindgut detoxification by the
233 microbiome.

234 First, we demonstrated that antibiotic treatment significantly impaired the
235 ability of *N. stephensi* to maintain body mass when feeding on juniper diets. These
236 results are consistent with studies demonstrating that reduction in the microbiota
237 impairs the ability of another woodrat species, *N. lepida*, to consume phenolic-rich
238 creosote resin (2), and the ability of pine weevils to thrive on terpene-rich diets
239 (21). It should be noted that antibiotic treatment can also have effects on host
240 physiology and gene expression (22). However, here we compared changes in food
241 intake and body mass in response to antibiotics of animals being fed either control
242 diets or juniper diets. Thus, both groups of animals were treated with antibiotics
243 and experienced the same effects due to the antibiotic treatment, but those feeding
244 on juniper exhibited greater declines in food intake and body mass. Based on these
245 results, it is clear that the gut microbiota plays an important role in detoxification
246 when juniper is consumed by *N. stephensi*.

247 Next, we compared concentrations of PSCs along the length of the
248 gastrointestinal tract. We predicted that if toxins were metabolized early in the gut,
249 their concentrations in the foregut chamber would be lower than those measured in
250 food material, similar to what has been observed for usnic acid in the reindeer
251 rumen (5). This was observed in the case of oxalate, where foregut concentrations
252 were roughly a third of those measured in the diet. Since oxalate is detected only at
253 very low levels in the urine of woodrats (16) and mammals do not produce the
254 necessary oxalate-degrading enzymes (23), it seems that oxalate is detoxified

255 efficiently by microbes in the foregut. Conversely, terpene concentrations in the
256 foregut were the same as those measured in food material, suggesting that the
257 foregut is not a significant site for detoxification. Instead, concentrations of terpenes
258 were lowest in the cecum, where some terpene compounds were not even detected.
259 These results are similar to those observed in sage-grouse, where terpene
260 concentrations are also lowest in the cecal chambers (24). *Neotoma stephensi* has
261 physiological adaptations that reduce terpene absorption in the gut (25), perhaps
262 allowing terpene metabolism to be delayed until the food reaches the cecum. In the
263 case of terpenes, concentrations increased in the large intestine compared to the
264 cecum. While this change seems puzzling, we hypothesize that the selective
265 absorption of water in this gut region results in higher concentrations of toxins.
266 Further experiments, perhaps using radiolabeled compounds, are needed to
267 understand the routes of absorption and detoxification of these compounds in
268 different regions of the woodrat digestive system.

269 Interestingly, we did not observe many differences related to detoxification
270 between the foregut microbial metagenomes of *N. stephensi* and *N. albigula*, even
271 though these two host species feed on different diets with contrasting chemical
272 profiles. It could be that the foregut microbiome offers broad detoxification
273 capacities, while cecal microbial communities are more specialized. That being said,
274 we did observe a higher abundance of enoyl-CoA hydratase in the foregut of *N.*
275 *stephensi* compared to *N. albigula*. This gene plays a role in the ability for microbes
276 to degrade terpenes (26), and is enriched in the gut metagenomes of sage-grouse (7)

277 and mountain pine beetles (20). Thus, there does seem to be some functional
278 enrichment for detoxification in the foregut of *N. stephensi*.

279 Within *N. stephensi*, the foregut and cecal microbial communities appear to
280 provide different detoxification functions. In the foregut, we observed higher
281 abundance of the gene 4-oxalocrotonate tautomerase, which is involved in the
282 degradation of aromatic hydrocarbons by bacteria (27). The foregut also had higher
283 abundances of the gene oxalyl-CoA decarboxylase, which degrades oxalate, and aryl-
284 alcohol dehydrogenase, which degrades aromatic hydrocarbons. The abundance of
285 aryl-alcohol dehydrogenase increases in the foregut of another woodrat species (*N.*
286 *lepida*) when animals are fed diets containing phenolic PSCs (2) and thus may be an
287 important enzyme that is provided by the foregut microbial community .

288 We also obtained evidence for enrichment of detoxification enzymes in the
289 cecal chamber. Higher-level gene categories, such as 'Drug Metabolism' and
290 'Chloroalkane and Chloroalkene Degradation' were more abundant in the cecal
291 chambers than the foregut. Specifically, the cecum was enriched for genes such as
292 hydroxyatrazine ethylaminohydrolase, which deaminates or dechlorinates triazine
293 compounds (28, 29), and anthraniloyl-CoA monooxygenase, which plays a role in
294 the catabolism of aromatic compounds (30). Additionally, the aldehyde
295 dehydrogenase gene was significantly more abundant in the cecum. This gene is
296 annotated as a component of the 'Limonene and Pinene Degradation' pathway, and
297 is found to be enriched in the gut metagenomes of sage-grouse (7) and mountain
298 pine beetles (20).

299 We found that the frequencies of genes encoding enzymes that are predicted
300 to function in benzoate degradation was conserved between gut chambers.
301 Benzoate degradation is hierarchically classified into xenobiotic degradation and
302 metabolism pathways. Benzoate degradation was classified as a conserved function
303 between both chambers due to both the similar frequency of this function in both
304 chambers as well as the observation that the bacterial lineages inferred to
305 contribute this function were found to have similar compositional profiles in both
306 chambers. Some of the eight genera observed in this group are well-known
307 ruminant symbionts (e.g. *Oxalobacter*), acidophiles (e.g. *Alicyclobacillus*), common
308 gut lineages (e.g. *Pseudomonas*), and chemoheterotrophs (*Sphingomonas)*. This
309 result suggests that overlapping components of microbiome communities in both
310 foregut and cecum are selected on the basis of their ability to contribute benzoate
311 degradation functions to the community.

312 Finally, we tested whether predictive profiling of metagenomics based on
313 16S rRNA sequences is appropriate for woodrat gut samples. We found a significant
314 relationship between the relative abundances of functional categories as estimated
315 by PICRUSt and determined by metagenomic sequencing. Additionally, results for
316 PICRUSt and metagenomics were consistent for some of the categories that
317 exhibited the largest differences between the two chambers. However, PICRUSt did
318 not predict all of the categories accurately. Many functional categories (e.g.
319 'Peptidases' and ''Amino acid Related Enzymes') were predicted to be present by
320 PICRUSt analysis, but were not detected by metagenomic sequencing. Interestingly,
321 the gut microbial communities of herbivores tend to have lower abundances of

322 genes encoding protease relative to carnivores, likely to conserve these nutrients on
323 a low protein diet (31). Thus, the use of predictive metagenomic profiling may not
324 always be feasible for non-model systems, especially given that most microbial
325 genomes used for predictive profiling are from the human gut. Indeed, PICRUSt
326 works significantly better for human samples than for samples from nonhuman
327 mammalian guts (32). The sequencing of additional genomes from nonhuman
328 mammals would help to improve the accuracy of programs like PICRUSt in non-
329 model systems. It seems that results from predicting profiling in non-model systems
330 should perhaps be verified with other methods, such as quantitative PCR.

331 Overall, we hypothesized that microbial detoxification should occur
332 proximally in the gastrointestinal tract, so as to facilitate degradation of PSCs before
333 they would be absorbed later in the gut. However, it seems that detoxification
334 processes may be spatially structured along the length of the gut. The evidence for
335 foregut detoxification is strongest for oxalate, where abundances of the
336 detoxification enzyme (oxalyl-CoA decarboxylase) were high, and concentrations of
337 oxalate were already much lower than in food material, and abundances of
338 potentially oxalate-degrading bacteria are highest (19). Terpene degradation may
339 occur in the cecal chamber, where abundances of terpene-degradation genes were
340 higher, and concentrations of terpenes were at their lowest. It is somewhat puzzling
341 why this spatial arrangement would exist, given that terpenes are absorbed very
342 rapidly due to their small size and high lipophilicity (25). However, *N. stephensi*
343 exhibits lower terpene absorption than other woodrat species (25), resulting in
344 relatively higher terpene exposure and resultant detoxification by microbial

345 communities in the hindgut. Laboratory rats are able to excrete ~25% of absorbed
346 monoterpenes back into the gut lumen through the biliary duct (33), an excretion
347 route that may be enhanced in a specialist herbivore such as *N. stephensi*. This
348 excretion route may facilitate further microbial degradation of terpenes in the
349 hindgut. While we did not measure concentrations of phenolics through the gut,
350 various genes associated with degrading aromatic hydrocarbons were enriched in
351 both the foregut and cecum. Phenolics can bind to dietary protein and digestive
352 enzymes, thus limiting nutrient availability (34). Therefore, foregut detoxification of
353 phenolics would be beneficial for avoiding the anti-nutritive effects of PSCs. Again,
354 labeled chemicals to trace sites of absorption, excretion, and metabolism would
355 enhance our understanding of the location of these processes.

356 The location of detoxification within the gut could have important ecological
357 and evolutionary implications for plants and herbivores. For example, when
358 comparing several species of rodents, only those with foregut chambers were able
359 to metabolize significant amounts of oxalate (35). Thus, evolution of this chamber
360 may be important for the ability to consume oxalate-rich plants. Consumption of
361 plant toxins might also drive changes in gut anatomy to enhance detoxification by
362 facilitating a longer duration of residency in various gut chambers. For example,
363 woodrats feeding on phenolic-rich oak exhibit an increase in cecal size (36), which
364 could be driven by increased fiber content of oak or to facilitate the detoxification of
365 PSCs. Interestingly, supplementing diets with isolated phenolic compounds causes
366 an increase in cecal size in lab rats (37). Alterations of the size or function of gut
367 chambers in response to toxins could have implications for dietary niche breadth or

368 energetics. In herbivorous birds, there is evidence suggesting that microbial
369 detoxification occurs in both foregut (6) and hindgut chambers (7). The guts of birds
370 are under strong selective pressure to be small so as to facilitate flight (38), and thus
371 sites of microbial detoxification may be especially important in these species.
372 Studies on additional and phylogenetically diverse herbivores and classes of PSCs
373 may help us to better understand the importance of microbial detoxification in the
374 gut, and how the spatial arrangement of these processes contribute to animal
375 morphology, performance, ecology, and evolution.
376

377 **MATERIALS AND METHODS**

378 *Antibiotic Feeding Trial*

379 We conducted a feeding trial coupled with antibiotic treatment to investigate
380 whether microbial communities contribute to the tolerance of a juniper-based diet.
381 Individuals of *N. stephensi*, as well as juniper foliage for diet experiments, were
382 collected from near Wupatki National Monument, AZ, USA (35°30' N, 111°27' W).
383 Animals were brought to the University of Utah animal facility and fed a diet of 50%
384 ground juniper and 50% rabbit chow for 3 days. Juniper diets (*J. monosperma*) were
385 prepared as previously described (25). Animals were then divided into either a
386 'Control Diet' group or a 'Juniper Diet' group, with four individuals in each group.
387 Animals in the Control diet group were transitioned to a juniper free diet by feeding
388 them a diet of 25% juniper/75% rabbit chow for 3 days, followed by 100% rabbit
389 chow for 6 days. Animals in the 'Juniper Diet' group were transitioned to an

390 increasing amount of juniper by feeding them a diet of 75% juniper/25% rabbit
391 chow for 3 days and then 90% juniper/10% rabbit chow for 6 days.

392 For the duration of the experiment, animals were given water containing
393 sucralose (2.5% w/v) to facilitate drinking. During the last 3 days of the experiment,
394 an antibiotic (0.5 g neomycin L^{-1}) was also added to the water of all animals.
395 Neomycin is a broad spectrum antibiotic that is poorly absorbed across the gut
396 tissue and reduces gut bacterial density by ~90% (39). This treatment has
397 effectively been used to demonstrate that gut microbes are critical for the ability of
398 another woodrat species, *N. lepida*, to consume phenolic-rich creosote resin (2).

399 Body mass was measured daily over the course of the experiment. The mass
400 of wet food presented was measured daily, and subsamples were used to estimate
401 the dry weight of the diet. On the following day, leftover food was collected, dried
402 overnight at 40°C and weighed to measure intake. Food intake was calculated as the
403 dry mass of food presented – dry mass of leftover food recovered.

404 We calculated the percent change in food intake and body mass between the
405 day prior to the beginning of antibiotic treatment to the end of the feeding trial.
406 These percentages were compared between the two groups using t-tests. This
407 feeding trial and all experiments below were approved by the University of Utah
408 Institutional Animal Care and Use Committee (IACUC) under protocols #12-12010
409 and #16-02011.

410

411 *Toxin Levels Throughout the Gut*

412 We conducted a feeding trial on *N. stephensi* to document changes in toxin
413 concentrations across gut regions. Six individuals of *N. stephensi* were fed increasing
414 concentrations of *J. monosperma* (3 days on 25%, 3 days on 50%, 4 days on 75%).
415 On the last morning, animals were euthanized using isoflurane. Contents of each gut
416 region (foregut, stomach, small intestine, cecum, large intestine, feces) were
417 collected. A small portion of wet gut contents were placed in airtight headspace
418 autosampler vials and frozen at -20°C until analysis. Concentrations of individual
419 monoterpenes were determined using headspace gas chromatography with an
420 Agilent 7694 headspace sampler coupled with an Agilent 6890N gas chromatograph
421 (GC). One mL of headspace gas was injected into a J&W DB-5 capillary column (30
422 m × 250 μm × 0.25 μm). Operating conditions for the headspace sampler were: oven
423 temperature at 100°C, loop temperature at 110°C, transfer line temperature at
424 120°C, a vial equilibrium time of 20 min, a pressurization time of 0.20 min, a loop fill
425 time of 0.50 min, a loop equilibrium time of 0.20 min, and an injection time of 0.50
426 min. Operating conditions for the GC were: splitless injector at 250°C, flame
427 ionization detector at 300°C, oven temperature at 40°C for 2 min, then increasing
428 3°C/min to 60°C, then increasing 5°C/min to 120°C, then increasing 20°C/min to
429 300°C, and held at 300°C for 7 min. The make-up gas was nitrogen and the carrier
430 gas was helium. The inlet pressure was 80 kPa with a flow rate of 1.0 mL/min.
431 Retention times and peak areas of individual monoterpenes were calculated using
432 Agilent OpenLab version A.01.05. We verified the relative retention times of
433 individual monoterpenes using standards, and estimated the relative concentrations
434 of individual monoterpenes in the intestinal content material by comparing AUC of

435 peaks in diet or gut samples to AUC of a known volume of 10 mg/mL monoterpene
436 standards.

437 Remaining gut contents were placed in weighing boats and dried at 40°C for
438 two nights. The dried gut contents were then used to measure oxalate
439 concentrations using a previously established protocol (40). Roughly 0.4g of dried
440 gut contents were ground and added to 5 mL of 6 N H_2SO_4 to solubilize the oxalate.
441 After 15 min, 25 ml of distilled water was added, and the entire solution was filtered
442 through grade 4 Whatman filter paper. The filtrate was brought up to a pH of 7 with
443 NaOH, and 0.1 g of $CaCl_2$ was added to precipitate the oxalate. The samples were
444 centrifuged and decanted. After centrifugation, a volume of distilled water equal to
445 that recovered after filtration was added, and the samples were titrated.

446

447 *Sample collection for metagenomics*

448 We compared the metagenomic sequencing results across species and gut
449 regions to investigate differential abundance of microbial functions. We collected
450 individuals of the cactus specialist *N. albigula*, from Castle Valley, UT, USA (38°30' N,
451 109°18' W). Additional individuals of *N. stephensi* were collected from near Wupatki
452 National Monument, AZ, USA (35°30' N, 111°27' W). Animals were immediately
453 transported back to the University of Utah animal facility, provided with native
454 diets: either cactus pads or juniper overnight (for *N. albigula* and *N. stephensi*,
455 respectively), and euthanized and dissected on the following morning. Contents of
456 the foregut chamber were collected from three individuals of both species, and the
457 contents of the cecal chamber were collected from *N. stephensi*. We sequenced the

458 metagenome of each sample (described below), and conducted several comparisons.
459 First, we compared the foregut metagenomes of *N. albigula* and *N. stephensi*, with
460 the prediction that the foregut of *N. stephensi* would be enriched in genes associated
461 with detoxification of juniper, which contains more chemical classes of defensive
462 compounds than cactus. Second, we compared the metagenomes of foregut contents
463 and cecal contents in *N. stephensi* with the prediction that the abundance of
464 detoxification genes would be higher in the foregut to facilitate detoxification prior
465 to the major site of absorption in the small intestine.
466
467 *Comparative metagenomics*
468 Total DNA was isolated from foregut and cecal contents using MoBio
469 PowerFecal DNA extraction kit (MoBio, Carlsbad, California). Extracted DNA was
470 sent to Argonne National Laboratory for sequencing. Genomic DNA was sheared
471 using a Covaris Sonicator, to roughly 150 bp and metagenomic shotgun libraries
472 were prepared using the Illumina TruSeq DNA sequencing preparation kits.
473 Libraries were sequenced on the Illumina HiSeq2000 platform using a 2 x 100 bp
474 run and V3 chemistry, which resulted in overlapping sequences.
475 Metagenomic sequences were uploaded to the MG-RAST website (41).
476 Sequences were screened against the genome of *Arabidopsis thaliana* to remove
477 potential contamination from the plant-based diet. The reads were then filtered
478 using dynamic trimming with a quality threshold of 15, such that any sequences
479 with more than 5 low-quality bases were removed. Several foregut metagenomes
480 contained high abundances of sequences (~30-50%) identified as plant DNA, likely

481 resulting from the diet. Therefore, we partitioned our analysis by domain by
482 selecting sequences identified as bacteria using the non-redundant multi-source
483 protein annotation database, M5nr (42). Abundances of non-plant eukaryotic and
484 archaeal sequences were too low for sufficient analysis. Sequences identified as
485 bacterial in origin were then annotated to identify putative functions using the
486 KEGG Orthology database (43, 44) with the following thresholds: (1) e-values < 1e-
487 5, (2) a minimum percent identity to database sequences of 60% and (3) a minimum
488 alignment length of 15 bases. We compared the abundances at Level 3 of the KEGG
489 hierarchical classification, as well as specific genes associated with "Xenobiotic
490 degradation and metabolism", "Geraniol degradation", and "Limonene and pinene
491 degradation". Abundances of functional categories were compared using JMP 12.0
492 (SAS Institute Inc.) using t-tests and the robust Response Screening function, which
493 performs the Benjamini-Hochberg false discovery rate (FDR) correction for multiple
494 tests (45).

495 We also conducted specific comparisons of the abundances of several
496 detoxification genes: oxalyl-CoA decarboxylase, aryl alcohol dehydrogenase, and
497 several genes associated with terpene metabolism. The gene oxalyl-CoA
498 decarboxylase (*oxc*) degrades the compound oxalate. The gene aryl alcohol
499 dehydrogenase is upregulated in the woodrat foregut when individuals are fed diets
500 containing phenolic-rich resin from creosote bush (2). Last, a number of genes
501 associated with the "Limonene and pinene degradation" are enriched or present in
502 the gut microbiota of specialist insect and avian herbivores that feed on terpene-rich
503 plants (7, 20). We compared the abundances of these genes using JMP 12.0 (SAS

504 Institute Inc.) using pairwise t-tests (foregut *N. stephensi* vs. foregut *N. albigula*, and
505 *N. stephensi* foregut vs. cecum) with the Dunn's correction.
506
507 *Metagenome prediction*
508 We also conducted microbial inventories by sequencing the variable regions
509 1-3 of 16S rRNA gene following experimental and bioinformatic methods described
510 in detail elsewhere (46). Taxonomic comparison of the communities between
511 foregut and cecal chambers has already been conducted with larger sample sizes
512 (11). In the current study, we used 16S rRNA inventories to predict the
513 metagenomic content of gut samples using genomic inference via PICRUSt (32). We
514 compared the relative abundances of functional categories between the shotgun
515 metagenomic and predicted metagenomics to assess if predictive profiling via
516 PICRUSt is informative for woodrat gut samples. First, we averaged the relative
517 abundances of functional categories within a sample type (foregut and cecum), and
518 transformed the relative abundances using a log(x+1) transformation. We then
519 conducted a linear regression between transformed PICRUSt abundances and
520 metagenomic abundances. We also plotted the relative abundances of functional
521 categories that exhibited the highest fold difference between the foregut and cecal
522 chambers to qualitatively inspect whether trends were similar for PICRUSt and
523 metagenomic data. We next investigated how variation in structure of the microbial
524 community across foregut and cecum was related to variation in functional
525 abundances across these sites. Using a comparative statistical framework
526 implemented in the R package FunkyTax (46) we classified functions into functional

527 community categories (enhanced, divergent, conserved, equivalent; see Phillips et
528 al. 2017, for further detail) resulting from the assessment of how similarities or
529 differences in functional frequency were compositionally derived between sites. The
530 significance of functional assignment rates to community categories were assessed
531 as binomial probabilities where the observed success rate was the frequency of a
532 function-category assignment, and the expected success rate was the study-wide
533 frequency of the function. False discovery was controlled with a Benjamini-
534 Hochberg p-value adjustment.

535 *Accession Numbers*

536 Metagenomic sequences can be found in the NCBI Short Read Archive (SRA)
537 database under BioProject PRJNA336354, and on MG-RAST under Metagenome
538 Project IDs mgp10174 and mgp10296. 16S rRNA sequences from the foregut and
539 cecal chambers of N. stephensi, which were used to PICRUSt analyses can be found
540 in the SRA database under BioProject PRJNA449358.

541

542

543 **Acknowledgements** – We would like to thank Madelina James and KayLene
544 Yamada for helping with feeding trials and Chelsea Merriman for analysis of
545 monoterpenes. Funding for this study was provided by the National Science
546 Foundation (Doctoral Dissertation Improvement Grant, DEB 1210094, to M.D.D. and
547 K.D.K.; DEB 1342615 to M.D.D.; DEB-1146194 to JSF; and DBI 1400456 to K.D.K).

548

549
550

551 **References**

552

553 1. Dearing MD, Foley WJ, McLean S. 2005. The influence of plant secondary
554 metabolites on the nutritional ecology of herbivorous terrestrial vertebrates
555 Ann Rev Ecol Evol Syst 36:169-185.
556 2. Kohl KD, Weiss RB, Cox J, Dale C, Dearing MD. 2014. Gut microbes of
557 mammalian herbivores facilitate intake of plant toxins. Ecol Lett 17:1238-
558 1246.
559 3. Hume ID, Warner ACI. 1980. Evolution of microbial digetion in mammals, p
560 665-684. *In* Ruckebusch Y, Thivend P (ed), Digestive Physiology and
561 Metabolism in Ruminants. MTD Press, Lancaster.
562 4. Mackie RI. 2014. Mutualistic fermentative digestion in the gastrointestinal
563 tract: diversity and evolution. Integr Comp Biol 42:319-326.
564 5. Sundset MA, Barboza PS, Green TK, Folkow LP, Blix AS, Mathiesen SD. 2010.
565 Microbial degradation of usnic acid in the reindeer rumen.
566 Naturwissenschaften 97:273-278.
567 6. Garcia-Amado MA, Michelangeli F, Gueneau P, Perez ME, Dominguez-Bello
568 MG. 2007. Bacterial detoxification of saponins in the crop of the avian foregut
569 fermenter *Opisthocomus hoazin*. J Anim Feed Sci 16:82-85.
570 7. Kohl KD, Connelly JW, Dearing MD, Forbey JS. 2016. Microbial detoxification
571 in the gut of a specialist avian herbivore, the Greater Sage-Grouse. FEMS
572 Microbiol Lett 363:fnw144.
573 8. Osawa R. 1992. Tannin-protein complex-degrading enterobacteria isolated
574 from the alimentary tracts of koalas and a selective medium for their
575 enumeration. Appl Environ Microbiol 58:1754-1759.
576 9. Clauss M, Frey R, Kiefer B, Lechner-Doll M, Loehlein W, Polster C, Rössner GE,
577 Streich WJ. 2003. The maximum attainable body size of herbivorous
578 mammals: morphophysiological constraints on foregut, and adaptations of
579 hindgut fermenters. Oecologia 136:14-27.
580 10. Alexander RM. 1991. Optimization of gut structure and diet for higher
581 vertebrate herbivores. Phil Trans R Soc 333:249-255.
582 11. Kohl KD, Miller AW, Marvin JE, Mackie R, Dearing MD. 2014. Herbivorous
583 rodents (*Neotoma* spp.) harbour abundant and active foregut microbiota.
584 Environ Microbiol 16:2869-2878.
585 12. Vaughan TA. 1982. Stephen's woodrat, a dietary specialist. J Mammal 63:53-
586 62.
587 13. Schwartz CC, Nagy JG, Regelin WL. 1980. Juniper oil yield, terpenoid
588 concentration, and antimicrobial effects on deer. J Wildl Manage 44:107-113.
589 14. Dearing MD, McLister JD, Sorensen JS. 2005. Woodrat (*Neotoma*) herbivores
590 maintain nitrogen balance on a low-nitrogen, high-phenolic forage, *Juniperus*
591 *monosperma*. J Comp Physiol B 175:349-355.
592 15. Holechek JL, Munshikpu L, Saiwana L, Nunez-Hernandez G, Valdez R, Wallace
593 JD, Cardenas M. 1990. Influences of six shrub diets varying in phenol content
594 on intake and nitrogen retention by goats. Trop Grassl 24:93-98.

595 16. Justice KE. 1985. Oxalate digestibility in *Neotoma albigula* and *Neotoma*
596 *mexicana*. Oecologia 67:231-234.
597 17. Miller AW, Oakeson KF, Dale C, Dearing MD. 2016. Microbial community
598 transplant results in increased and long-term oxalate degradation. Microb
599 Ecol 72:470-478.
600 18. Miller AW, Dale C, Dearing MD. 2017. The induction of oxalate metabolism in
601 vivo is more effective with functional microbial communities than with
602 functional microbial species. mSystems 2:e00088-17.
603 19. Miller AW, Kohl KD, Dearing MD. 2014. The gastrointestinal tract of the
604 white-throated woodrat (Neotoma albigula) harbors distinct consortia of
605 oxalate-degrading bacteria. Appl Environ Microbiol 80:1595-1601.
606 20. Adams AS, Aylward FO, Adams SM, Erbilgin N, Aukema BH, Currie CR, Suen G,
607 Raffa KF. 2013. Mountain pine beetles colonizing historical and naive trees
608 are associated with a bacterial community highly enriched in genes
609 contributing to terpene metabolism. Appl Environ Microbiol 79:3468-3475.
610 21. Berasategui A, Salem H, Paetz C, Santoro M, Gershenzon J, Kaltenpoth M,
611 Schmidt A. 2017. Gut microbiota of the pine weevil degrades conifer
612 diterpenes and increases insect fitness. Mol Ecol 26:4099-4110.
613 22. Morgun A, Dzutsev A, Dong X, Greer RL, Sexton DJ, Ravel J, Schuster M, Hsiao
614 W, Matzinger P, Shulzhenko N. 2015. Uncovering effects of antibiotics on the
615 host and microbiota using transkingdom gene networks. Gut 64:1732-1743.
616 23. Miller AW, Dearing MD. 2013. The metabolic and ecological interactions of
617 oxalate-degrading bacteria in the mammalian gut. Pathogens 2:636-652.
618 24. Kohl KD, Pitman E, Robb BC, Connelly JW, Dearing MD, Forbey JS. 2015.
619 Monoterpenes as inhibitors of digestive enzymes and counter-adaptations in
620 a specialist avian herbivore. J Comp Physiol B 185:425-434.
621 25. Sorensen JS, Turnbull CA, Dearing MD. 2004. A specialist herbivore (*Neotoma*
622 *stephensi*) absorbs fewer plant toxins than does a generalist herbivore
623 (*Neotoma albigula*). Physiol Biochem Zool 77.
624 26. Iurescia S, Marconi AM, Tofani D, Gambacorta A, Paternò A, Devirgiliis C, van
625 der Werf MJ, Zennaro E. 1999. Identification and sequencing of β-myrcene
626 catabolism genes from *Pseudomonas* sp. strain M1. Appl Environ Microbiol
627 65:2871-2876.
628 27. Harayama S, Timmis KN. 1989. Catabolism of aromatic hydrocarbons by
629 *Pseudomonas*, p 152-175. *In* Hopwood DA, Chater KF (ed), Genetics of
630 Bacterial Diversity. Academic Press, London.
631 28. Boundy-Mills K, de Souza ML, Mandelbaum RM, Wackett LP, Sadowsky MJ.
632 1997. The atzB gene of *Pseudomonas* sp. strain ADP encodes the second
633 enzyme of a novel atrazine degradation pathway. Appl Environ Microbiol
634 63:916-923.
635 29. Seffernick JL, Shapir N, Schoeb M, Johnson G, Sadowsky MJ, Wackett LP. 2002.
636 Enzymatic degradation of chlorodiamino-s-triazine. Appl Environ Microbiol
637 68:4672-4675.
638 30. Carmona M, Zamarro MT, Blázquez B, Durante-Rodríguez G, Juárez JF,
639 Valderrama JA, Barragán MJ, Garcia JL, Díaz E. 2009. Anaerobic catabolism of

640 aromatic compounds: a genetic and genomic view. Microbiol Mol Biol Rev
641 73:71-133.
642 31. Muegge BD, Kuczynski J, Knights D, Clemente JC, González A, Fontana L,
643 Henrissat B, Knight R, Gordon JI. 2011. Diet drives convergence in gut
644 microbiome functions across mammalian phylogeny and within humans.
645 Science 332:970-974.
646 32. Langille MGI, Zaneveld J, Caporaso JG, McDonald D, Knights D, Reyes JA,
647 Clemente JC, Burkepile DE, Thurber RLV, Knight R, Beiko RG, Huttenhower C.
648 2013. Predictive functional profiling of microbial communities using 16S
649 rRNA marker gene sequences. Nat Biotechnol 31:814-821.
650 33. Igimi H, Nishimura M, Kodama R, Ide H. 1973. Studies on the metabolism of
651 d-limonene (p-mentha-1,8-diene): I. the absorption, distribution and
652 excretion of d-limonene in rats. Xenobiotica 4:77-84.
653 34. Min BR, Barry TN, Attwood GT, McNabb WC. 2003. The effect of condensed
654 tannins on the nutrition and health of ruminants fed fresh temperate forages:
655 a review. Anim Feed Sci Technol 106:3-19.
656 35. Shirley EK, Schmidt-Nielsen K. 1967. Oxalate metabolism in the pack rat,
657 sand rat, hamster, and white rat. J Nutr 91:496-502.
658 36. Skopec MM, Haley S, Torregrossa A-M, Dearing MD. 2008. An oak (Quercus
659 agrifolia) specialist (*Neotoma macrotis*) and a sympatric generalist (Neotoma
660 lepida) show similar intakes and digestibilities of oak. Physiol Biochem Zool
661 81:426-433.
662 37. Zduńczyk Z, Juśkiewicz J, Estrella I. 2006. Cecal parameters of rats fed diets
663 containing grapefruit polyphenols and inulin as single supplements or in a
664 combination. Nutrition 22:898-904.
665 38. Price ER, Brun A, Caviedes-Vidal E, Karasov WH. 2015. Digestive adaptations
666 of aerial lifestyles. Physiol 30:69-78.
667 39. Vijay-Kumar M, Aitken JD, Carvalho FA, Cullender TC, Mwangi S, Srinivasan S,
668 Sitaraman SV, Knight R, Ley RE, Gewirtz AT. 2010. Metabolic syndrome and
669 altered gut microbiota in mice lacking Toll-like receptor 5. Science 328:228-
670 231.
671 40. Miller AW, Oakeson KF, Dale C, Dearing MD. 2016. Effect of dietary oxalate on
672 the gut microbiota of the mammalian herbivore *Neotoma albigula*. Appl
673 Environ Microbiol 82:2669-2675.
674 41. Meyer F, Paarmann D, D'Souza M, Olson R, Glass EM, Kubal M, Paczian T,
675 Rodriguez A, Stevens R, Wilke A, Wilkening J, Edwards RA. 2008. The
676 metagenomics RAST server–a public resource for the automatic phylogenetic
677 and functional analysis of metagenomes. BMC Bioinformatics 9:386.
678 42. Wilke A, Harrison T, Wilkening J, Field D, Glass EM, Kyrpides N, Mavrommatis
679 K, Meyer F. 2012. The M5nr: a novel non-redundant database containing
680 protein sequences and annotations from multiple sources and associated
681 tools. BMC Bioinformatics 13:141.
682 43. Kanehisa M, Sato Y, Kawashima M, Furumichi M, Tanabe M. 2016. KEGG as a
683 reference resource for gene and protein annotation. Nucleid Acids Res
684 44:D457-D462.

44. Kanehisa M, Goto S. 2000. KEGG: Kyoto Encyclopedia of Genes and Genomes. Nucleid Acids Res 28:27-30.
45. Benjamini Y, Hochberg Y. 1995. Controlling the false discovery rate: a practical and powerful approach to multiple testing. J R Soc Stat Soc B 57:289-300.
46. Phillips CD, Hanson J, Wilkinson JE, Koenig L, Rees E, Webala P, Kingston T. 2017. Microbiome structural and functional interactions across host dietary niche space. Integr Comp Biol 57:743-755.

728 **Figure Legends**

729

730 **Fig. 1.** Changes in food intake and body mass as a result of antibiotics (AB). Bars
731 represent means ± 1 s.e.m.

732

733 **Fig. 2.** Concentrations of water and toxins across gut regions. The dotted line on
734 toxin graphs represents concentrations as measured in the food material presented
735 to woodrats. Points represent means ± 1 s.e.m.

736

737 **Fig. 3.** Functional categories (KEGG Level 3) that differed significantly between the
738 foregut metagenomes of *N. albigula* and *N. stephensi.* Bars represent means ± 1
739 s.e.m.

740

741 **Fig 4.** Differences in the metagenomic content of the foregut and cecal chambers of
742 *N. stephensi.* Bars represent means ± 1 s.e.m. A) Functional categories (KEGG Level
743 3) that differed significantly in abundance between the foregut and cecal
744 metagenomes. B) Detoxification genes that differed significantly in abundance
745 between the foregut and cecal metagenomes.

746

747 **Fig. 5.** Relative abundances of specific detoxification enzyme genes associated with
748 *a priori* hypotheses from other systems (see Methods). Bars represent means ± 1
749 s.e.m. Relative abundances were compared using t-tests (foregut *N. stephensi* vs.
750 foregut *N. albigula*, and *N. stephensi* foregut vs. cecum) with the Dunn's correction.

751 **Fig. 6. A)** A comparison of predictive profiling by PICRUSt and metagenomic data.
752 **B)** Bar graphs depict the functional categories that exhibited the highest fold-
753 differences between the foregut and cecal metagenomes. Bars represent means ± 1
754 s.e.m.
755

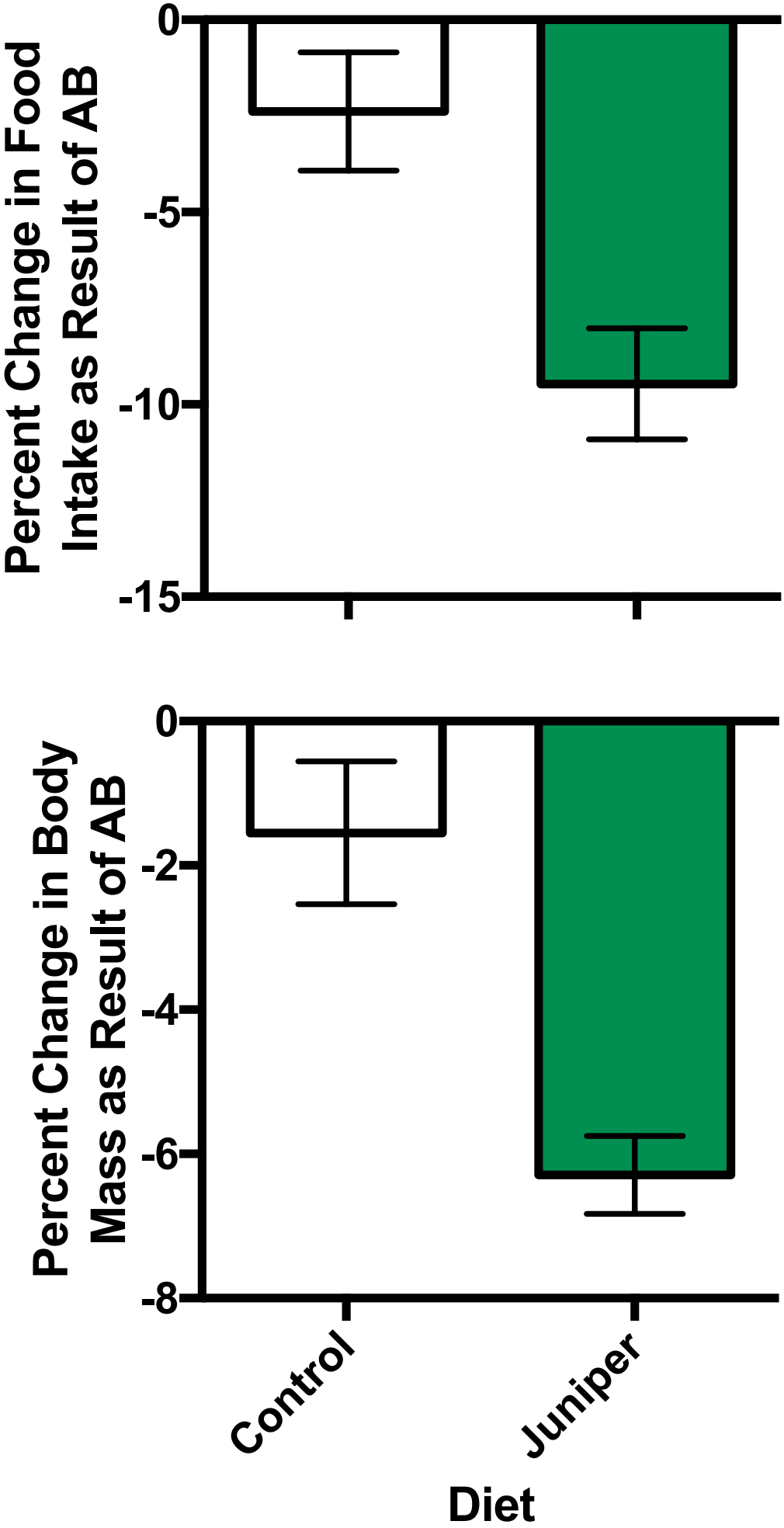
Percent Change in Food Intake as Result of AB
0
-5
-10
-15
Percent Change in Body Mass as Result of AB
0
-2
-4
-6
-8
Control
Juniper
Diet

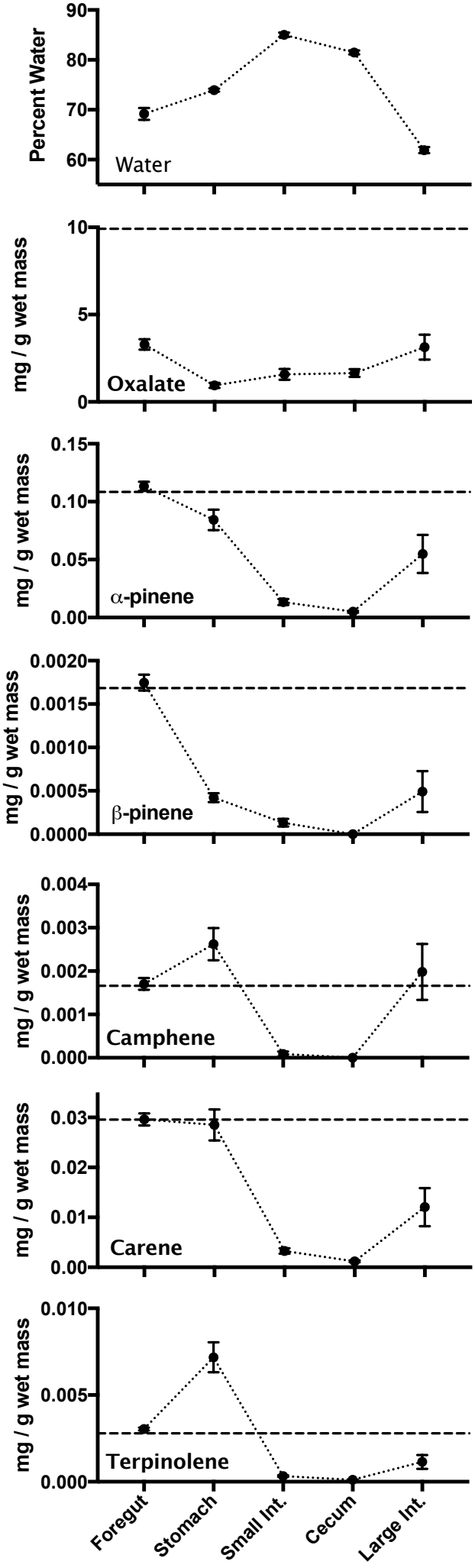
Percent Water
90
80
70
60
Water
mg / g wet mass
10
5
0
Oxalate
mg / g wet mass
0.15
0.10
0.05
0.00
α-pinene
mg / g wet mass
0.0020
0.0015
0.0010
0.0005
0.0000
β-pinene
mg / g wet mass
0.004
0.003
0.002
0.001
0.000
Camphene
mg / g wet mass
0.03
0.02
0.01
0.00
Carene
mg / g wet mass
0.010
0.005
0.000
Terpinolene
Foregut
Stomach
Small Int.
Cecum
Large Int.

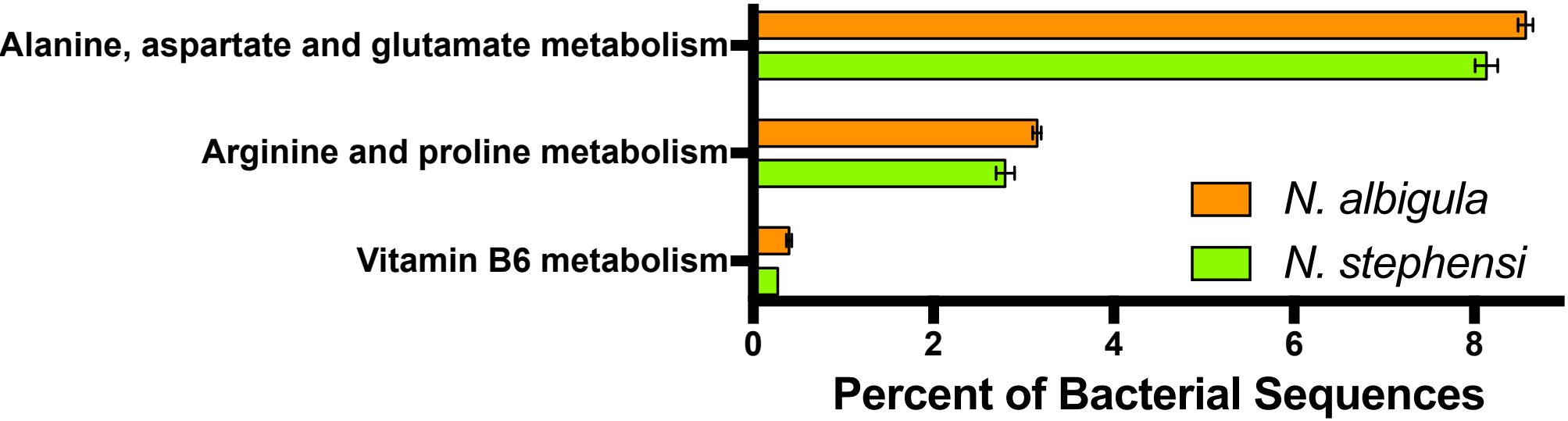
Alanine, aspartate and glutamate metabolism
Arginine and proline metabolism
Vitamin B6 metabolism
N. albigula
N. stephensi
0
2
4
6
8
Percent of Bacterial Sequences

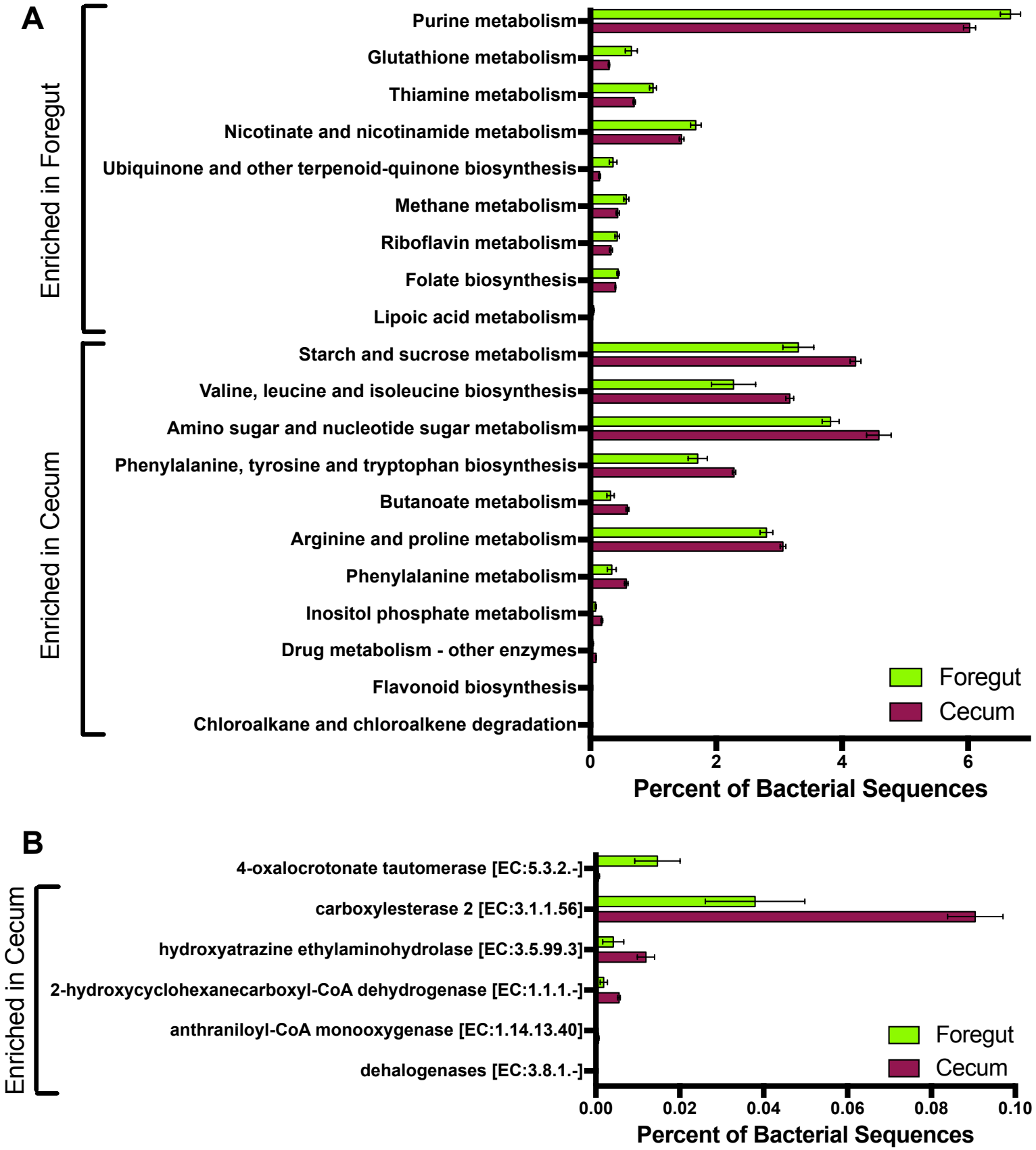
A
Enriched in Foregut
Purine metabolism
Glutathione metabolism
Thiamine metabolism
Nicotinate and nicotinamide metabolism
Ubiquinone and other terpenoid-quinone biosynthesis
Methane metabolism
Riboflavin metabolism
Folate biosynthesis
Lipoic acid metabolism
Enriched in Cecum
Starch and sucrose metabolism
Valine, leucine and isoleucine biosynthesis
Amino sugar and nucleotide sugar metabolism
Phenylalanine, tyrosine and tryptophan biosynthesis
Butanoate metabolism
Arginine and proline metabolism
Phenylalanine metabolism
Inositol phosphate metabolism
Drug metabolism - other enzymes
Flavonoid biosynthesis
Chloroalkane and chloroalkene degradation
Foregut
Cecum
0
2
4
6
Percent of Bacterial Sequences
B
Enriched in Cecum
4-oxalocrotonate tautomerase [EC:5.3.2.-]
carboxylesterase 2 [EC:3.1.1.56]
hydroxyatrazine ethylaminohydrolase [EC:3.5.99.3]
2-hydroxycyclohexanecarboxyl-CoA dehydrogenase [EC:1.1.1.-]
anthraniloyl-CoA monooxygenase [EC:1.14.13.40]
dehalogenases [EC:3.8.1.-]
Foregut
Cecum
0.00
0.02
0.04
0.06
0.08
0.10
Percent of Bacterial Sequences

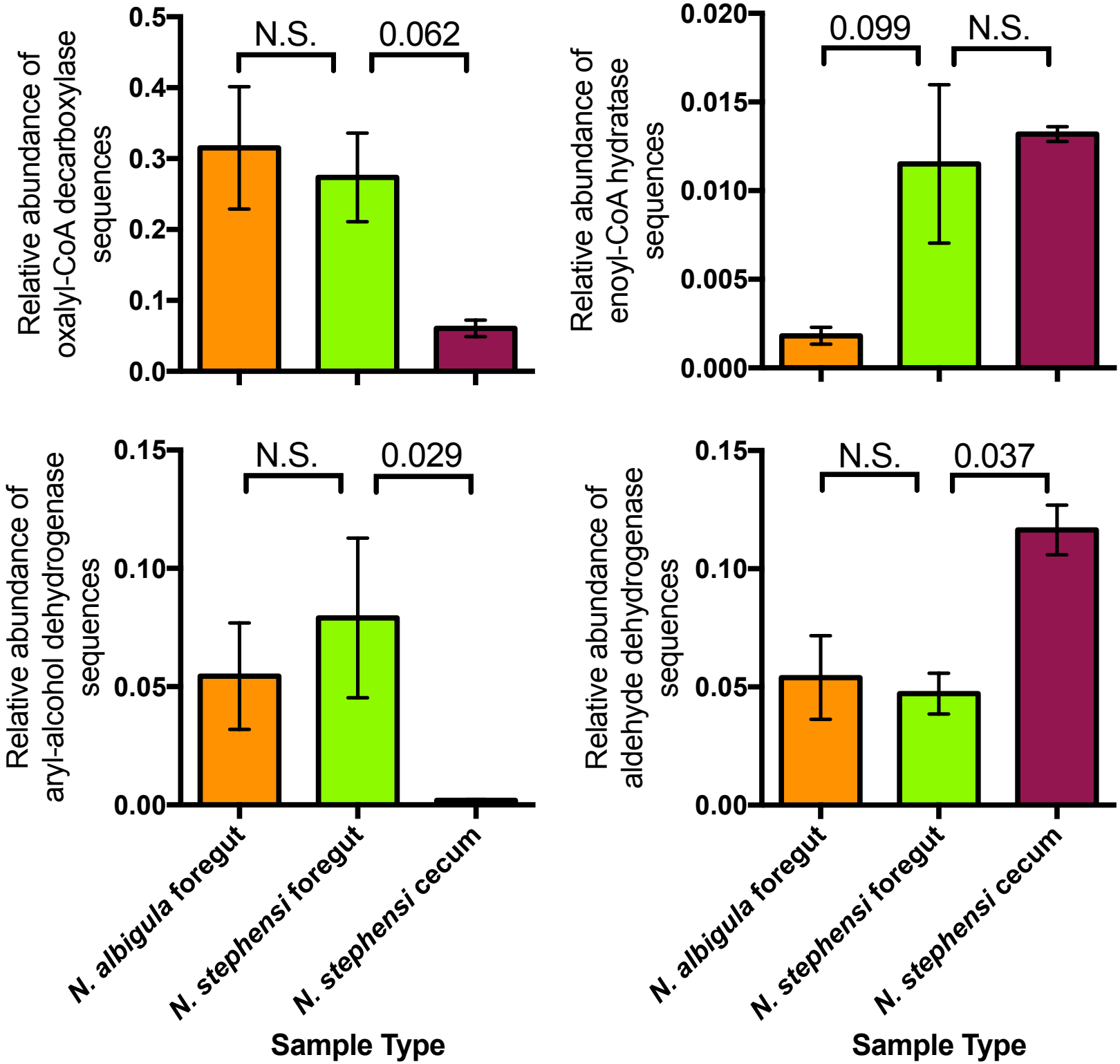
Relative abundance of oxalyl-CoA decarboxylase sequences
0.5
0.4
0.3
0.2
0.1
0.0
N.S.
0.062
Relative abundance of enoyl-CoA hydratase sequences
0.020
0.015
0.010
0.005
0.000
0.099
N.S.
Relative abundance of aryl-alcohol dehydrogenase sequences
0.15
0.10
0.05
0.00
N.S.
0.029
Relative abundance of aldehyde dehydrogenase sequences
0.15
0.10
0.05
0.00
N.S.
0.037
N. albigula foregut
N. stephensi foregut
N. stephensi cecum
Sample Type
N. albigula foregut
N. stephensi foregut
N. stephensi cecum
Sample Type

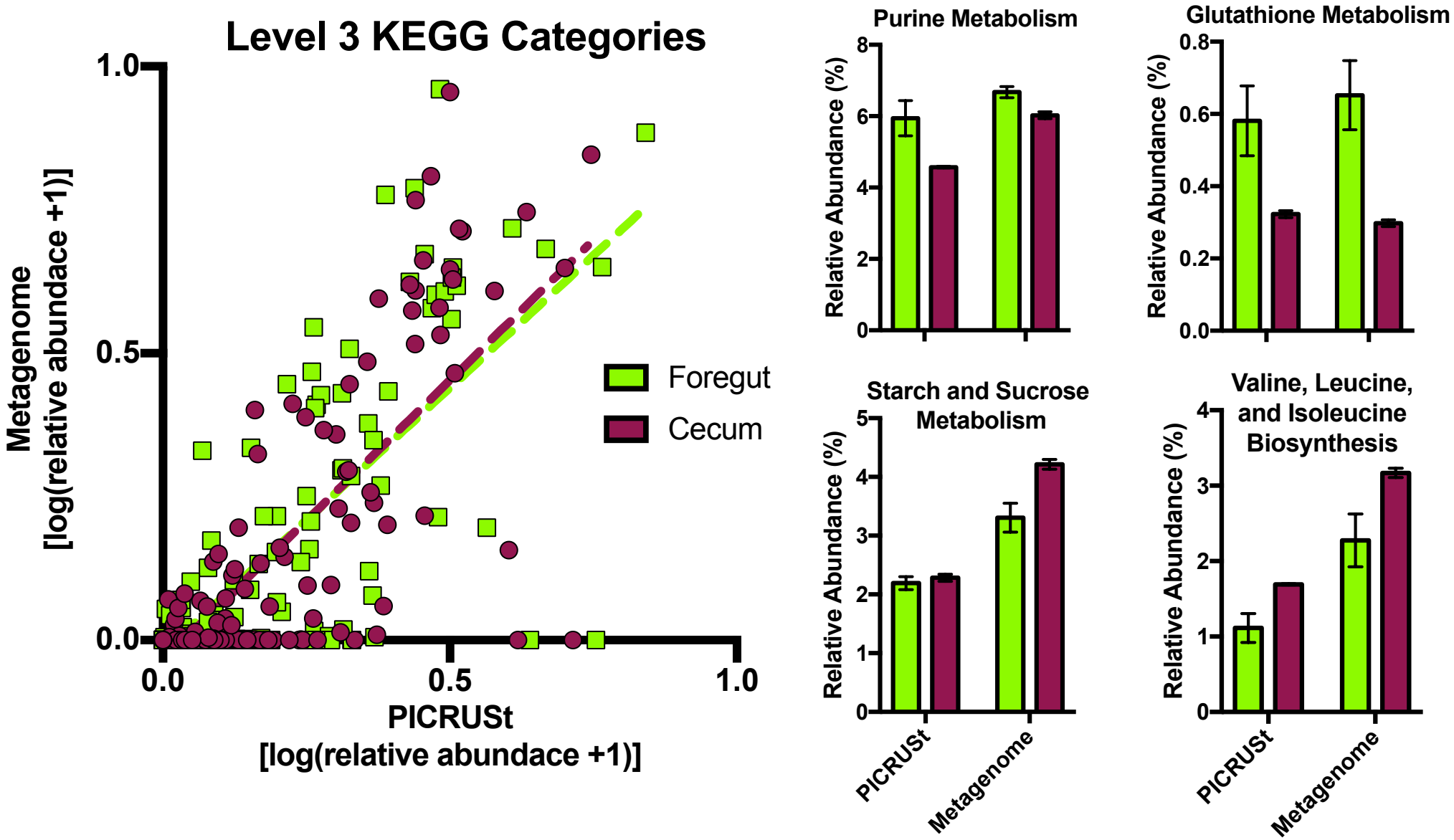
Level 3 KEGG Categories
Metagenome
[log(relative abundace +1)]
PICRUSt
[log(relative abundace +1)]
0.0
0.5
1.0
Foregut
Cecum
Purine Metabolism
Glutathione Metabolism
Starch and Sucrose Metabolism
Valine, Leucine, and Isoleucine Biosynthesis
Relative Abundance (%)
PICRUSt
Metagenome